Materials Research Bulletin 87 (2017) 114–118

Contents lists available at ScienceDirect

Materials Research Bulletin

journal homepage: www.elsevier.com/locate/matresbu

Hydrothermal synthesis of In_2O_3-loaded $BiVO_4$ with exposed {010}{110} facets for enhanced visible-light photocatalytic activity

Qiongjun Liu, Yan Liu, Bifen Gao, Yilin Chen, Bizhou Lin*

Department of Applied Chemistry, College of Materials Science and Engineering, Huaqiao University, Xiamen 361021, PR China

ARTICLE INFO

Article history:
Received 17 August 2016
Received in revised form 5 November 2016
Accepted 8 November 2016
Available online 23 November 2016

Keywords:
A. Semiconductors
A. Inorganic compounds
B. Solvothermal
D. Catalytic properties

ABSTRACT

Under the strategies of the morphology engineering method and the heterojunction construction, $In_2O_3/BiVO_4$ composites with different molar ratios were prepared through a simple two-step hydrothermal route. The as-prepared monoclinic $BiVO_4$ showed a truncated bipyramid shape with high exposed {010}{110} facets, on which the hexagonal In_2O_3 nanoparticles were grown, leading to the formation of a heterojunction structure. Due to the high-active exposure facets of $BiVO_4$ and the improved photogenerated carriers separation efficiency of the formed heterojunction, $In_2O_3/BiVO_4$ exhibited excellent visible-light photocatalytic activity in the degradation of rhodamine B.

1. Introduction

Visible-light photocatalysis has attracted remarkable interest, reflecting that it can harvest more energy from the incoming solar energy offers a desirable way to solve energy and environmental issues [1,2]. The process of semiconductor-based photocatalysis in a heterogeneous system involves the generation, migration, and separation of electron–hole pairs [3]. However, up to now, the efficiency of photocatalysis is still too low for practical applications. One disastrous drawback is the fast recombination of photo-induced electron-hole pairs. It was reported that constructing semiconductor heterojunction structures can increase the charge separation efficiency [2,4].

Recently, monoclinic bismuth vanadate (m-$BiVO_4$) with a bandgap of about 2.4 eV has been widely investigated [5–7]. It was demonstrated that m-$BiVO_4$ with high exposed {010}{110} facets has high activity [8–10]. However, the efficiency of m-$BiVO_4$ is relative low owing to its poor charge transport characteristics and weak surface adsorption properties [11,12]. To improve its photocatalytic efficiency, researchers found that the introduction of oxide semiconductor materials to fabrication heterojunctions with $BiVO_4$ can inhibit the fast recombination of the photogenerated carriers and enhance the photocatalytic efficiency [8,13–15]. Hexagonal and cubic indium oxides (h- and c-In_2O_3) with bandgaps of ~3.0 eV are candidates in the photocatalytic degradation of organic pollutants [16]. The energy band alignments of In_2O_3 and m-$BiVO_4$ are well matched. It is expected that In_2O_3 is a suitable material to fabricate a new heterojunction structure with m-$BiVO_4$ for enhancing the separation efficiency of the photogenerated carriers. In 2015, Jian et al. employed the one-pot hydrothermal method to prepare c-In_2O_3/m-$BiVO_4$ heterostructured composites with high visible-light photocatalytic activity [14], in which the as-obtained m-$BiVO_4$ particles showed a disordered morphology. Under the strategies of the morphology engineering method and the heterojunction construction, in this work, we synthesized m-$BiVO_4$ particles with high-active {010}{110} exposure facets via a simple hydrothermal route. Subsequently, the heterostructured $In_2O_3/BiVO_4$ composites, in which h-In_2O_3 nanoparticles were grown on the surfaces of m-$BiVO_4$ through a facile solvothermal approach. The as-prepared $In_2O_3/BiVO_4$ composites exhibited enhanced visible-light photocatalytic activity in the degradation of a model dye (rhodamine B, RhB).

2. Experimental

2.1. Preparation of $In_2O_3/BiVO_4$ heterojunctions

All chemicals were of analytical reagent grade and used without further purification. $BiVO_4$ was synthesized by a hydrothermal route. 0.36 mmol $Bi(NO_3)_3\cdot 5H_2O$ and 0.36 mmol NH_4VO_3 were dissolved into 8 mL of 2 M HNO_3 solution and 22 mL of 2 M $NH_3\cdot H_2O$ solution, respectively. After violent stirring for 30 min, the NH_4VO_3 solution was added drop-wise into the $Bi(NO_3)_3$ solution. And the pH of the mixed solution was adjusted to 0.6 using $NH_3\cdot H_2O$ solution and kept stirring for 2 h. The resultant mixture was transferred into a 100-mL Teflon-lined stainless-steel

---

* Corresponding author.
E-mail addresses: bzlin@hqu.edu.cn, bzlinhqu@126.com (B. Lin).

http://dx.doi.org/10.1016/j.materresbull.2016.11.012
0025-5408/

autoclave, and then was heated to and maintained at 200 °C for 24 h. After cooling, a yellow powder was centrifugalized, washed with water and ethanol for three times, and dried at 80 °C in a drying oven.

$In_2O_3/BiVO_4$ composites with different ratios were prepared under hydrothermal conditions with a fixed 0.1 mmol addition of the as-synthesized $BiVO_4$ and a fixed $In(NO_3)_3$:urea ratio (1:30). In a typical synthesis route for preparing $In_2O_3:BiVO_4 = 0.3:1$ (referred as S3 thereafter), 0.06 mmol $In(NO_3)_3$ and 1.8 mmol urea with 0.1 mmol $BiVO_4$ were dispersed in the mixture of 25 mL diethylene glycol and 10 mL water by ultrasonic vibrating for 1 h. The obtained mixture was transferred into a 50-mL autoclave, and then heated to and maintained at 180 °C for 24 h. After reaction, the precipitate was centrifugalized, washed with water for three times, and calcined at 450 °C for 2 h. The products were referred as S0.5 (for 0.010 mmol $In(NO_3)_3$ addition), S1 (0.02 mmol), S2 (0.04 mmol) and S3 (0.06 mmol), S4 (0.08 mmol), respectively. The pure In_2O_3 was also prepared by the same procedure without $BiVO_4$.

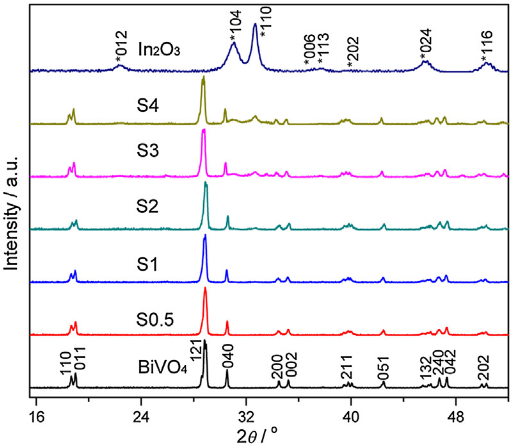

Fig. 1. XRD patterns of $In_2O_3/BiVO_4$ composites.

2.2. Characterization

The crystal structures were characterized by powder X-ray diffraction (XRD) using a Rigaku D/max-2500 diffractometer with Cu Kα radiation. The morphology was observed on a field emission scanning electron microscope (FE-SEM, Hitachi, SU-70) and a high resolution transmission electron microscope (HRTEM, JOEL JEM-2010). X-ray photoelectron spectroscopy (XPS) was carried out on a VGESCALAB MK II with an Al Kα X-ray source. The photocurrent responses were measured in Na_2SO_4 electrolyte (0.1 M) using the CHI660D electrochemical station in a conventional three-electrode configuration under visible light irradiation. UV–vis diffuse absorption spectra were recorded on a Shimadzu UV-2550 spectrophotometer using $BaSO_4$ as the reference.

2.3. Evaluation of photocatalytic activity

The activities of the photocatalysts were evaluated by the degradation of RhB aqueous solution under visible light irradiation, provided by A Changtuo 500W Xe arc lamp through a 10-cm IR water filter and a cutoff filter ($\lambda > 400$ nm). In a typical run, the experiment was carried out by adding 50 mg photocatalyst to 100 mL RhB solution with an initial concentration (5 mg/L). Before illumination, the mixture was stirred in dark for 30 min to ensure the adsorption–desorption equilibrium. At an irradiation interval of every 0.5 h, 4 mL suspension was collected and the RhB concentration was determined by measuring the maximum absorbance at 554 nm using a UV–vis spectrophotometer.

3. Results and discussion

The XRD patterns of samples are illustrated in Fig. 1. It clearly shows that all of them were well crystallized and the diffraction peaks could be assigned to monoclinic $BiVO_4$ (JCPDS 14-0688) and hexagonal In_2O_3 (JCPDS 22-0336). No other peaks were distinctly detected, indicating that the obtained samples are of high purity without impurity. The reflections for In_2O_3 in $In_2O_3/BiVO_4$ composites are intenser with increasing its amount.

Fig. 2a and b reveal that the morphology of the as-prepared $BiVO_4$ exhibits a truncated bipyramid shape with smooth clean surfaces and high exposed {010}{110} facets. As shown in Fig. 2c and d, the loaded In_2O_3 nanoparticles are evenly dispersed on the $BiVO_4$ surfaces. But it should be pointed out that some of the loaded In_2O_3 nanoparticles are hard agglomerated and that the peripheral In_2O_3 particles have no contact with $BiVO_4$. After several attempts, it was found that the hard agglomeration was inevitable under our preparation conditions. The lattice fringes of $BiVO_4$ and In_2O_3 can be clearly observed form the HRTEM image of $In_2O_3/BiVO_4$ (Fig. 2e). As shown in Fig. 2d and e, $BiVO_4$ and its surrounding In_2O_3 particles showed an intimate contact, leading to the formation of the $In_2O_3/BiVO_4$ heterojunction (Fig. 2f).

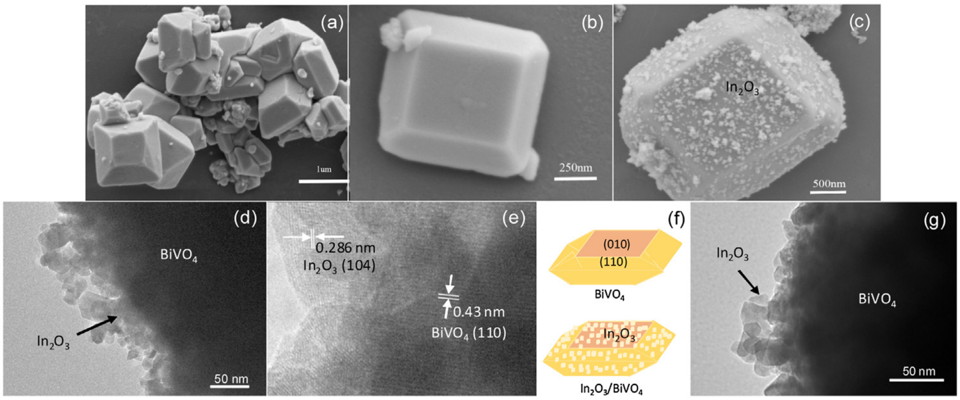

Fig. 2. FE-SEM images of $BiVO_4$ (a and b) and $In_2O_3/BiVO_4$ composite S3 (c), HRTEM images of $In_2O_3/BiVO_4$ composite (d and e), the illustrations of $BiVO_4$ and the $In_2O_3/BiVO_4$ heterojunction (f), and HRTEM image of $In_2O_3/BiVO_4$ composite after the photocatalytic reaction (g).